MANSOURA JOURNAL OF CHEMISTRY
Official Journal of Faculty of Science, Mansoura University, Egypt
E-mail: scimag@mans.edu.eg ISSN: 2974-4938

Synthesis, investigation, and biological activity of novel Zn(II) and Fe(III) complexes of cyanohydrazone derivatives ligand.

Marwa Sakr[1], Mohammed M. El-Gamil[1,2], Usama El-Ayaan[1], Gaber M. Abu El-Reash[1]*

[1]*Department of Chemistry, Faculty of Science, Mansoura University, El-Gomhoria Street, 35516 Mansoura, Egypt*

[2]*Department of Toxic and Narcotic Drug, Forensic Medicine, Mansoura Laboratory, Medico legal Organization, Ministry of Justice, Mansoura, Egypt*

Received:21/7/2025
Accepted:17/8/2025

Abstract: This study involves the synthesis and characterization of zinc(II) and iron(III) complexes of cyanohydrazone-based ligands (H_2L). The structure of the resulting chelates were elucidated through a combination of elemental analysis, magnetic measurements, Atomic Absorption (AAS), infrared spectroscopy, and UV-Vis techniques, offering insight into the coordination environment and geometry. Density Functional Theory (DFT) was applied to optimize and propose the most possible molecular geometries of both complexes and exhibits that the complex of zinc(II) had tetrahedral geometry, whereas the complex of Fe(III) had octahedral geometry. Thermal analysis of $[Zn(L)(H_2O)].0.5H_2O$ and $[Fe(HL)_2(H_2O)_2].Cl.2H_2O$ complexes was performed to investigate their decomposition behavior, from which kinetic and thermodynamic parameters were extracted using the Horowitz–Metzger and Coats–Redfern models. Furthermore, the synthesized compounds were screened for biological activities, including antioxidant potential using the 2,2- Diphenyl -1-picrylhydrazyl (DPPH) free radical method and antibacterial efficacy against selected microbial strains. The findings support promising bioactivity and stability profiles, offering potential applications in biomedical and pharmaceutical fields.

keywords: Cyanohydrazone , DFT, TGA , and biological activity

1.Introduction

Hydrazones are regarded as a significant family of organic compounds with two nitrogen species that are distinct from one another. They contain an azomethine group (−C=N-NH−)[1-3]. In contrast, A carbonyl group next to the -C=N- increases the hydrazide hydrazone's ability to coordinate with metal ions and form complexes. Moreover, the NH group and carbonyl activity enable this linker to act as a hydrogen-bond donor/acceptor, enhancing the compound's potential to bind to the desired targets in biology[4]. Hydrazine is condensed with an aldehyde or ketone to create hydrazones, which is accomplished with straightforward, manageable reagents[5, 6]. Hydrazone ligands can act as bridging or multidentate building blocks in structural assemblies by coordinating through atoms that donate electrons, such as nitrogen or oxygen[7]. When hydrazone coordinates with a metal ion, their activity usually increases. Due to a partial sharing of its positive charge with the donor atom located within the chelate ring system, coordination causes the metal ion to become more lipophilic. The core metal ion's increased lipophilicity makes it easier for it to penetrate the lipid membranes of bacteria or tumor cells, which accelerates up their death[8]. Hydrazones have a wide range of biological properties, including anticancer, antimicrobial[9], antifungal[10], and antioxidant properties[11]. This work aims to produce and analyze Zn(II) and Fe(III) complexes of Cyanohydrazone derivatives ligand (H_2L) using conventional and spectroscopic approaches. The geometry of the prepared compound was optimized using the DMOL3 module of the material studio program. They have also been tested for antibacterial, antifungal, and antioxidant properties.

2. Materials and Instrumentation

Every chemical and solvent used was acquired from reputable suppliers such as Sigma-Aldrich and Merck. A Mattson 5000 FTIR Spectrophotometer was used to record infrared spectra of KBr discs in the 4000–400 cm^{-1} range. Utilizing a Perkin-Elmer 2400 Series II analyzer, the contents of carbon, hydrogen, and nitrogen were measured. The complexes' metal contents were ascertained using Atomic Absorption spectroscopy (AAS). The electronic spectra were obtained using the Spectrophotometer (ATI UNICAM UV–Visible UV2). Thermogravimetric measurements (TGA, DTG, 20–800 °C) were carried out using a Shimadzu DTG-60H, nitrogen flow rate of 15 milliliters per minute and a heating rate of 10 degrees Celsius per minute in a thermogravimetric analyzer. At room temperature, all measurements were made.

2.1. Synthesis of complexes:

1 mmol of solid ligand Cyanohydrazon derivatives (H_2L) was refluxed with 1 mmol of $Zn(OAc)_2.2H_2O$ or $FeCl_3$ salt at 70 °C for 6 hours in presence of 15 ml absolute ethanol, the

precipitate was then isolated, filtered, washed, dried, and purity confirmed using TLC. Zn(II) complex (Figure1) is yellow color, with 88% yield, m.p > 300˚C, M.F. $C_{11}H_{12}ZnN_3O_{4.5}$, M.Wt = 323.61 g/mol, found (calculated) elemental analysis C= 40.95 (40.83), H=3.53 (3.74), N= 12.73(12.98), and Zn= 20.45 (20.25).

Fe(III) complex (Figure1) is brown color, with 78% yield, m.p = 276˚C, M.F. $C_{22}H_{28}ClFeN_6O_{10}$, M.Wt = 627.79 g/mol, found (calculated) elemental analysis C = 42.18 (42.09), H = 4.72 (4.50), N = 13.19 (13.39), Cl = 5.45 (5.65), and Fe = 8.96 (8.92).

2.2. Biological applications

2.2.1. Antimicrobial activity

We evaluated the antibacterial properties of $[Zn(L)(H_2O)]0.5H_2O$ and $[Fe(HL)_2(H_2O)_2]Cl.2H_2O$ chelates using the agar diffusion technique. Numerous varieties of bacteria were investigated[12].

2.2.2. DPPH test for antioxidant activity:

The DPPH• colorimetric technique with standard ascorbic acid was utilized to evaluate the antioxidant capacity of the compounds under investigation, as published[13]

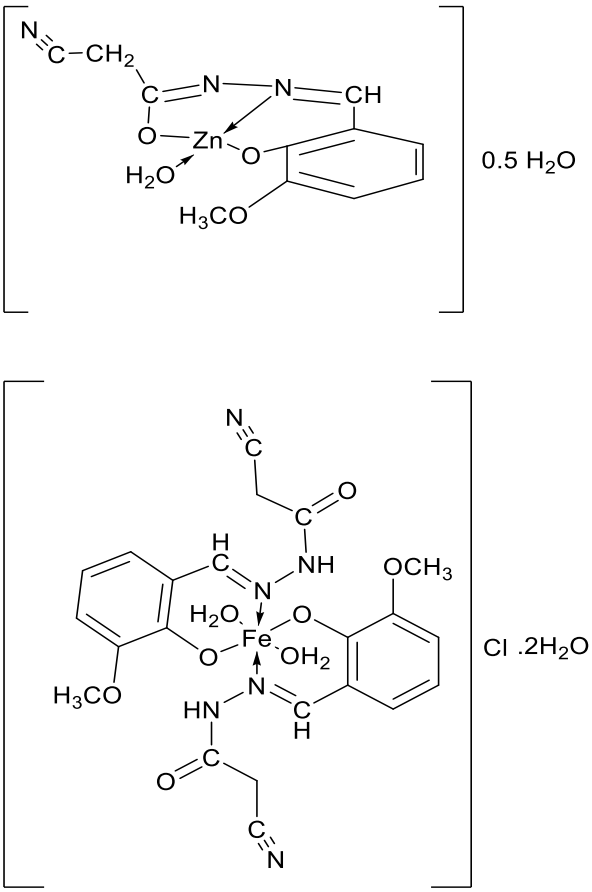

Fig (1): The structures of $[Zn(L)(H_2O)].0.5H_2O$ and $[Fe(HL)_2(H_2O)_2].Cl.2H_2O$ complex

3. Results and Discussion

3.1. IR Spectra (Figure 2):

For $[Zn(L)(H_2O)].0.5H_2O$ complex, The L ligand appears a binegative tridentate ONO ligand. The lack of the υ(N-H) and υ(C=O) vibrational bands and the concurrent appearance of bands at 1541 and 1111 cm^{-1} that are attributed to the new υ(C=N) group and υ(C-O) validate this coordination form. The change of υ(C=N) to a lower wavenumber indicates the involvement of the (C=N) groups in the complex creation process..

In the $[Fe(HL)_2(H_2O)_2]Cl.2H_2O$ complex the HL ligand coordinates to Fe(III) ions through the deprotonated (C-OH) groups of the phenolic ring and exhibits mononegative, bidentate ON behavior. By lowering the wavenumber of υ(C=N), the participation of the (C=N) azomethine groups in the complex formation process is confirmed. The chelation mode is validated by the lack of the υ(OH) band, as well as bands that show up at 3412 and 853 cm^{-1} correspond to the complex's

coordinated or non-coordinated water molecules. To establish that the water was crystalline and coordinated, TGA tests were performed.

3.2. Electronic spectra (Figure 3)**:**

The electronic spectra of Zn(II)-complex displays a wide band at roughly 21645 cm^{-1}, demonstrating LMCT. According to the d^{10} electronic configuration of Zn (II), the complex excluding these bands do not exhibit any notable transitions below this band[14].

The electronic spectra of Fe(III)-complex displays bands at 15384, 21367, and 25000 cm^{-1} that are ascribed to the $^6A_{1g} \rightarrow {}^4T_{1g}(G)$, $^6A_{1g} \rightarrow {}^4T_{2g}(G)$, and $^6A_{1g} \rightarrow {}^4Eg(G)$ transitions, respectively. These transitions are typical of an octahedral geometry surrounding the Fe(III) ion. The proposed shape of the Fe(III) complexes is additionally confirmed by the magnetic moment value (6.1 B.M.)[15].

Table 1: Physical and analytical information regarding metal complexes

Complex (empirical formula)	Mwt ($g\ mol^{-1}$)	Color	%found(%calc)				
			C	H	N	M	Cl
$C_{11}H_{12}ZnN_3O_{4.5}$	323.61	Yellow	40.95 (40.83)	3.53(3.74)	12.73(12.98)	20.45(20.25)	-
$C_{22}H_{28}ClFeN_6O_{10}$	627.79	Brown	42.18(42.09)	4.72(4.50)	13.19(13.39)	8.96(8.92)	5.45 5.65

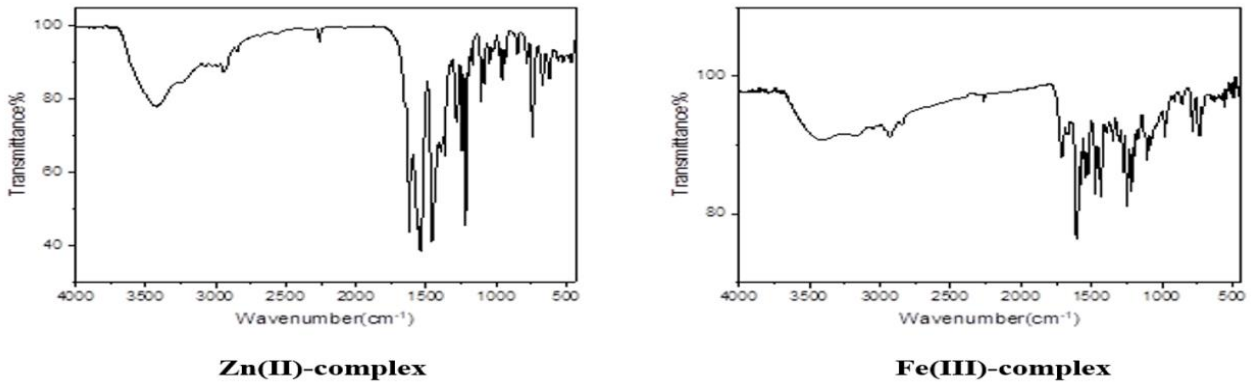

Figure 2: FT-IR Spectrum of Zn(II) and Fe(III) Complexes

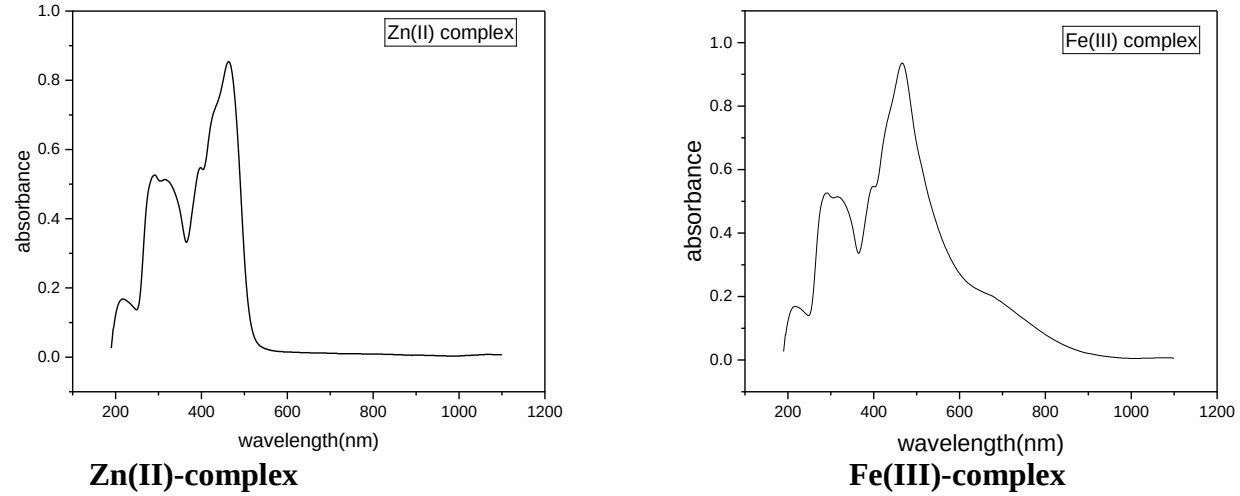

Figure 3: UV-vis. Spectra of **Zn(II)** and **Fe(III)** complexes

3.3. **Thermogravimetric & Kinetic Data Analysis (Table 2-4):**

The analysis using thermogravimetry TG and the thermogravimetric derivative (DTG) for the complexes $[Zn(L)(H_2O)].0.5H_2O$ and $[Fe(HL)_2(H_2O)_2].Cl.2H_2O$ were obtained. between 20 and 800 degrees Celsius (Figure 4).

For example, Zn(II)-complex the first stage which occurs between 25 and 119 °C, exhibits a reduction in weight 2.62 (calc 2.78%). The temperature range for the next phase was

between 119 and 265 °C., equal to one mole of H_2O (coordinated water) being lost 5.47 % (Calc 5.57%). The third breakdown process from 265 to 334°C involves the elimination of

C_2H_2N with a weight loss 12.50%(calc 12.38%), while the fourth step the elimination of $C_3H_5O_2$ causes weight reduction from 334 to 423°C 22.42% (calc 22.60%). The fifth breakdown stage occurs at temperatures ranging from 423-553°C, with a mass loss 24.55% (calc 24.14%) be attributable

to the elimination of $C_4H_2N_2$. yielding as the final product (2C and ZnO) with a mass of 32.43% (calc. 32.50%).

Figure 4 shows five stages of deterioration for $[Fe(HL)_2(H_2O)_2].Cl.2H_2O$. The first step involved the evaporation of the two hydrated water molecules at temperatures between 32 - 112 C (weight loss: found 6.27%; calc 5.74%). The second step, from 112 to 204 C, involved the removal of ($2H_2O$) (weight loss: found 6.07%; calc 5.74%). The third step, from 204 to 298 C, involved the removal of (HCl+HCN+CONH) (weight loss: found 16.73%; calc 16.98%). the fourth step, from 298 to 622 C, involved the removal of ($2HCN+C_{13}H_{11}N_2O_3$) (weight loss: found 47.01 %; calcd 47.36%). The fifth step, from 622 to 706 C, involved the removal of ($C_5H_4O_2$) (found 14.94%; calc 15.31%), and the final product (Fe) with a mass of 8.96% (calc. 8.93%).

Utilizing the Coats-Redfern and Horowitz-Metzger techniques (Figures 5 and 8), the kinetic parameters were ascertained[16, 17].

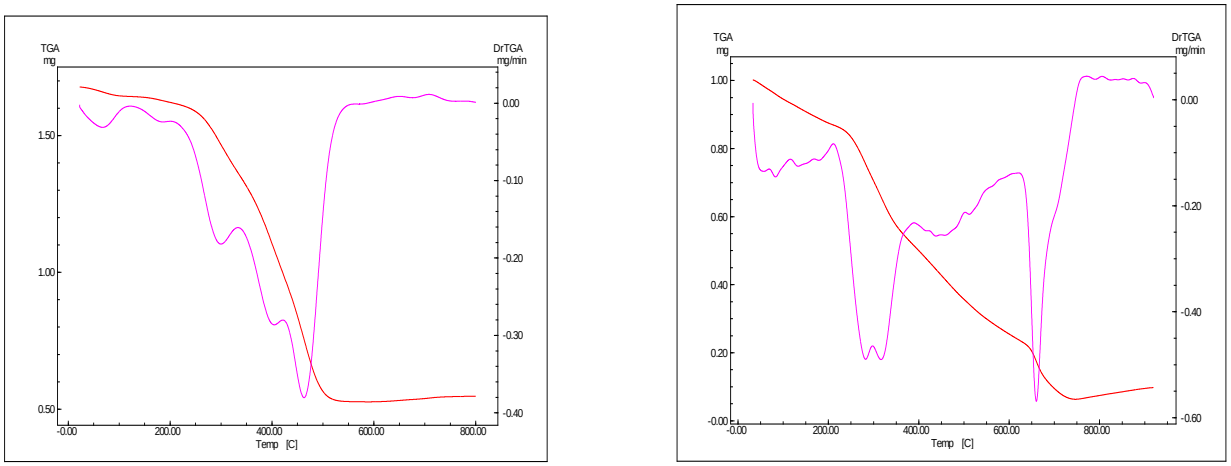

Zn(II)-complex **Fe(III)-complex**

Figure 4: (TGA, DrTGA) curves of Zn(II) and Fe(III) complexes.

Table 2: Decomposition steps for the compound.

Compound	Temp. range(°C)	Removed species	Wt.Loss	
			%found	%calculated
$[Zn(L)(H_2O)].0.5H_2O$ F. Wt. = 323.61	25-119	-($0.5H_2O$)	2.62	2.78
	119-265	-(H_2O)	5.47	5.57
	265-334	-(C_2H_2N)	12.50	12.38
	334-423	-($C_3H_5O_2$)	22.42	22.60
	423-553	-($C_4H_2N_2$)	24.55	24.14
	>553	-(ZnO+2C) Residue	32.43	32.50
$[Fe(HL)_2(H_2O)_2].Cl.2H_2O$ F. Wt. = 627.79	32-112	-($2H_2O$)	6.27	5.74
	112-204	-($2H_2O$)	6.07	5.74
	204-298	(HCl+HCN+CONH)	16.73	16.98
	298-622	($2HCN+C_{13}H_{11}N_2O_3$)	47.01	47.36
	622-706	-($C_5H_4O_2$)	14.94	15.31
	>706	-(Fe)Residue	8.96	8.93

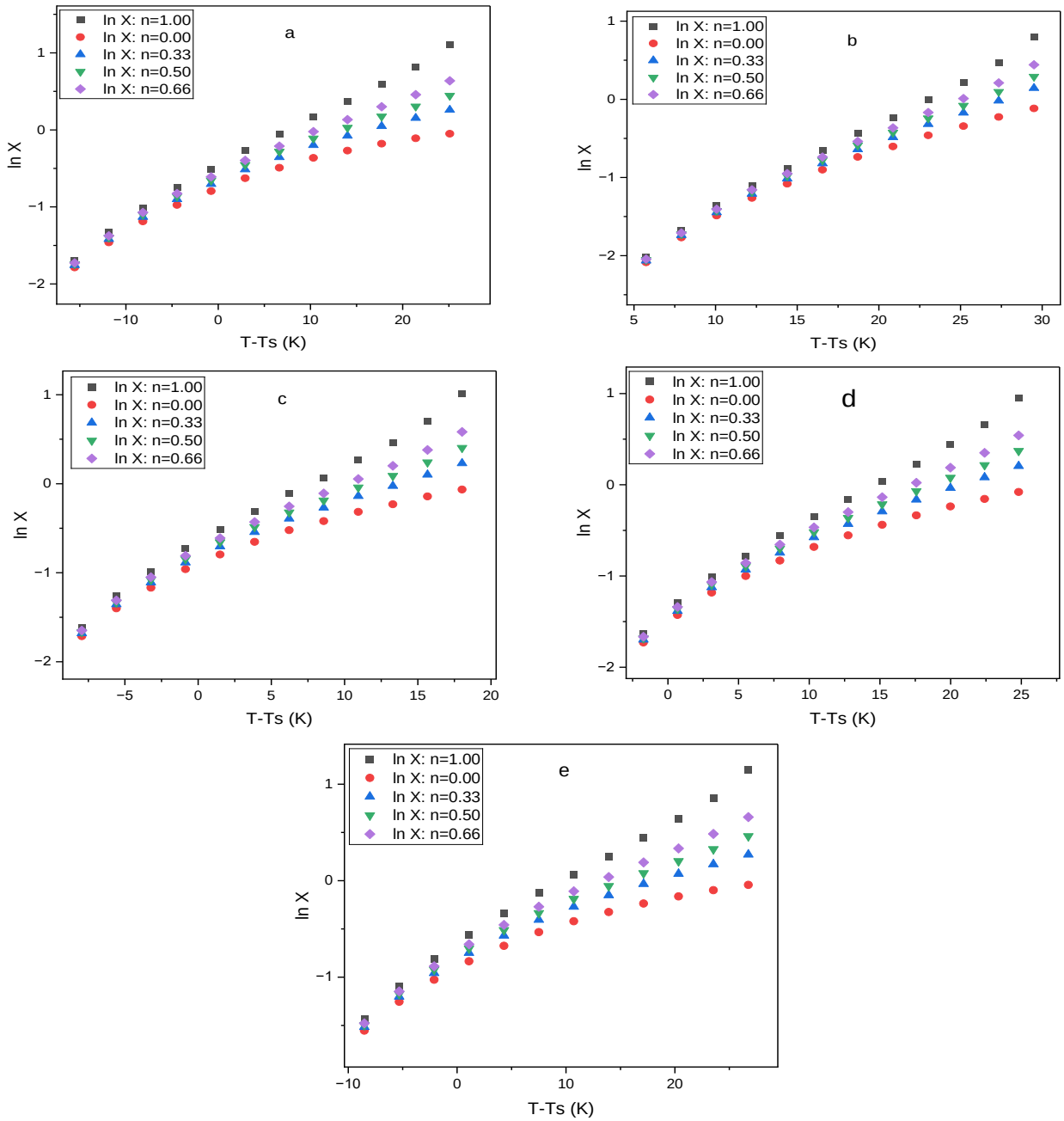

Figure 5: Horowitz- Metzger graphs illustrating the degradation stages of the [Zn(L)(H_2O)].0.5H_2O complex.

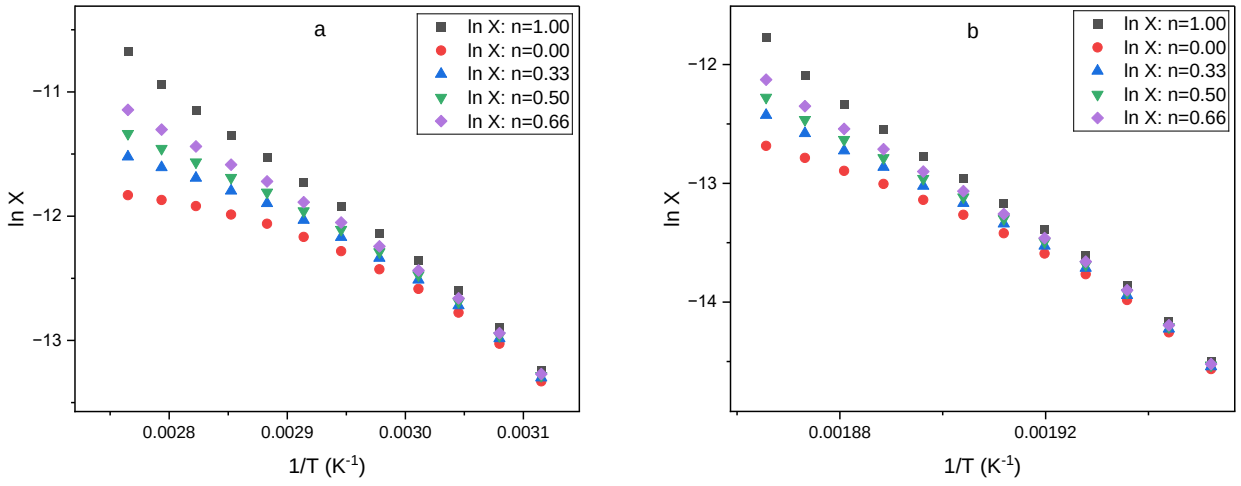

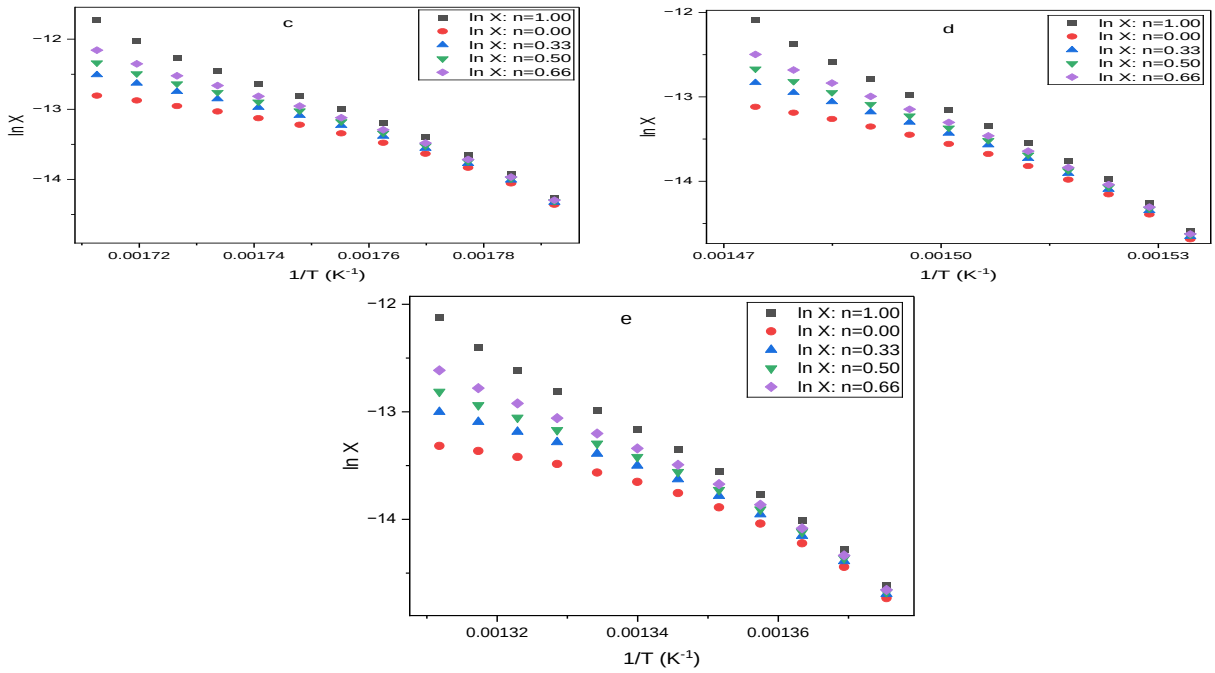

Figure 6: Coats-Redfern graphs illustrating the degradation stages of the $[Zn(L)(H_2O)].0.5H_2O$ complex.

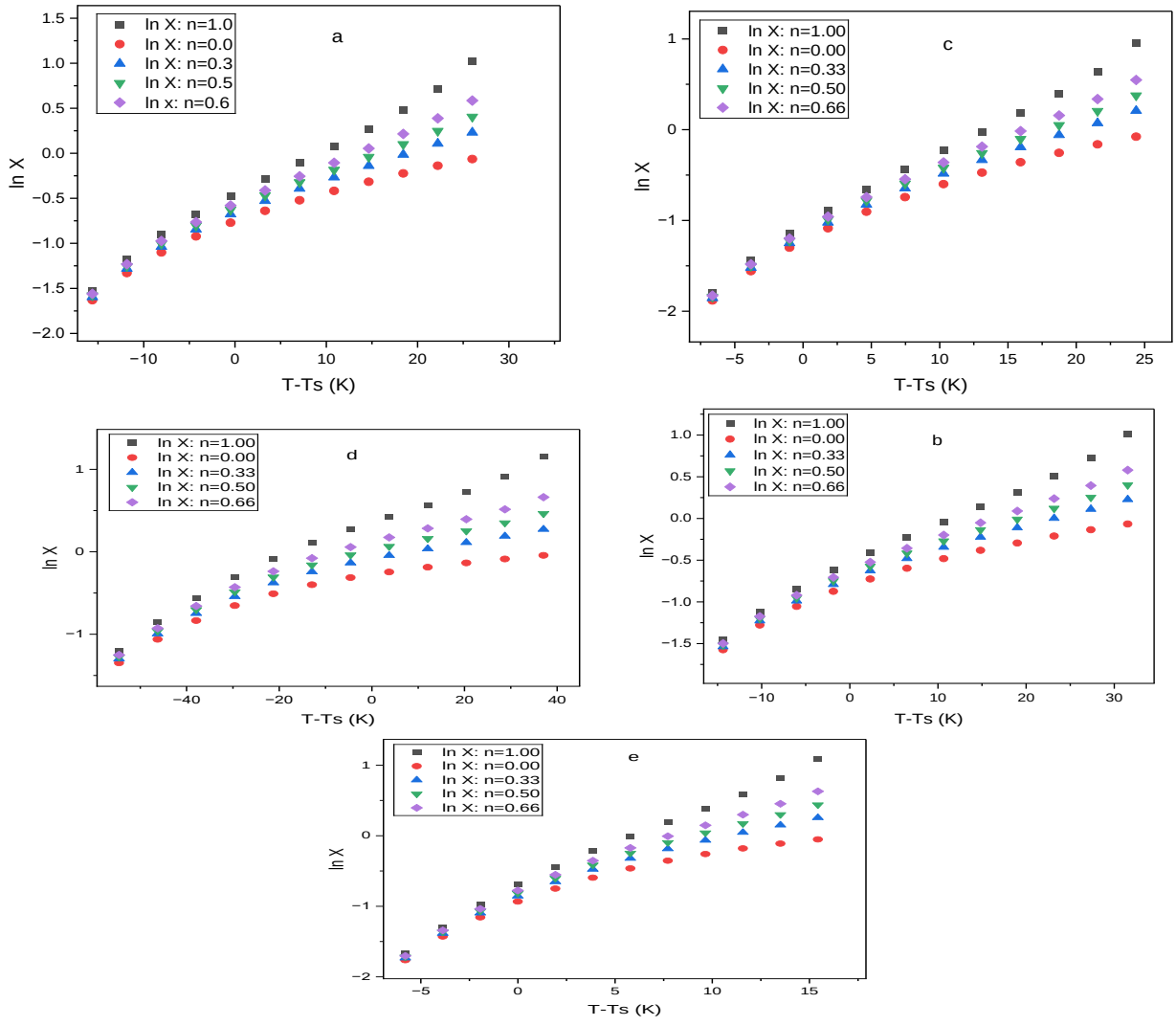

Figure 7: Horowitz- Metzger graphs illustrating the degradation stages of the $[Fe(HL)_2(H_2O)_2].Cl.2H_2O$ complex.

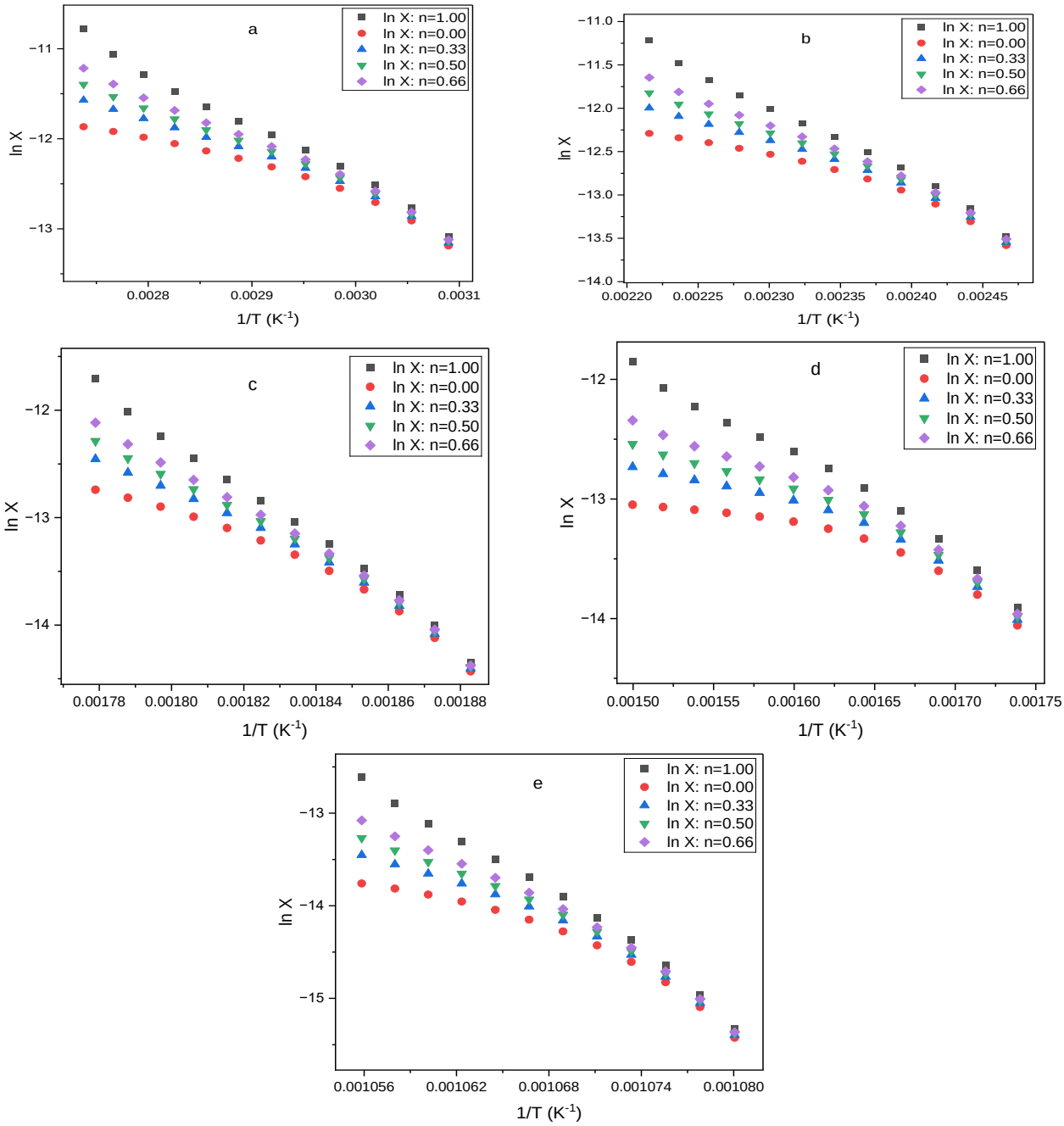

Figure 8: Coats-Redfern graphs illustrating the degradation stages of the $[Fe(HL)_2(H_2O)_2].Cl.2H_2O$ complex.

Table 3: Kinetic parameters for $[Zn(L)(H_2O)].0.5H_2O$ and $[Fe(HL)_2(H_2O)_2].Cl.2H_2O$ complexes were assessed using the Coats-Redfern equation.

Complex	Step	Mid Temp. (K)	E_a	A (S^{-1})	ΔH^* KJ\mol	ΔS^* KJ\mol	ΔG^* KJ\mol
$[Zn(L)(H_2O)].0.5H_2O$	1st	336.56	67.05	1.82×10^{8}	64.25	-0.0877	93.79
	2nd	506.5	275.60	3.33×10^{23}	271.39	0.2392	150.19
	3rd	565.88	284.72	1.52×10^{24}	280.01	0.2127	159.64
	4th	653.44	371.80	2.01×10^{27}	366.37	0.2712	189.10
	5th	735.58	354.12	8.46×10^{22}	348.01	0.1861	211.06
$[Fe(HL)_2(H_2O)_2]Cl.H_2O$	1st	339.28	58.26	5.90×10^{6}	55.44	-0.1163	94.91
	2nd	419.8	81.02	6.07×10^{7}	77.53	-0.0987	118.98
	3rd	537.75	227.00	5.22×10^{19}	222.53	0.1276	153.88
	4th	629.75	79.14	2.33×10^{4}	73.90	-0.1674	179.38
	5th	931.67	1024.4	2.61×10^{55}	1016.74	0.8065	265.34

Table 4: Kinetic parameters for $[Zn(L)(H_2O)].0.5H_2O$ and $[Fe(HL)_2(H_2O)_2].Cl.2H_2O$ complexes were assessed using the Horowitz-Metzger equation.

Complex	Step	Mid Temp. (K)	E_a	A (S^{-1})	ΔH^* KJ\mol	ΔS^* KJ\mol	ΔG^* KJ\mol
$[Zn(L)(H_2O)]0.5H_2O$	1st	336.56	72.05	1.02×10^{9}	69.25	-0.0734	93.97
	2nd	506.5	267.37	4.62×10^{24}	263.16	0.2228	150.27
	3rd	565.88	290.92	5.53×10^{24}	286.22	0.2234	159.77
	4th	653.44	371.82	1.96×10^{27}	366.39	0.2710	189.26
	5th	735.58	359.99	2.05×10^{23}	353.87	0.1938	211.26
$[Fe(HL)_2(H_2O)].Cl.2H_2O$	1st	339.28	63.304	3.31×10^{7}	60.483	-0.1020	95.093
	2nd	419.80	86.06	2.41×10^{8}	82.57	-0.0872	119.21
	3rd	537.75	230.43	1.07×10^{20}	225.96	0.1337	154.06
	4th	629.75	94.065	4.001×10^{5}	88.829	-0.1438	179.43
	5th	931.67	1032.4	7.17×10^{55}	1024.6	0.8149	265.46

3.4. Molecular modeling:

3.4.1. Geometry optimization:

(Figure 9 and 10) shows the optimized structures of the $[Zn(L)(H_2O)].0.5H_2O$ and $[Fe(HL)_2(H_2O)_2].Cl.2H_2O$ complexes. The complex $[Zn(L)(H_2O)].0.5H_2O$ had tetrahedral geometries, whereas the complex $[Fe(HL)_2(H_2O)_2].Cl.2H_2O$ had octahedral geometries.

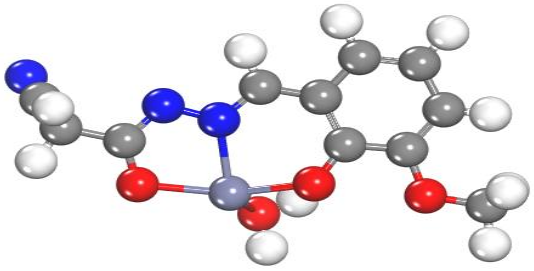

Figure 9: Molecular structure of $[Zn(L)(H_2O)].0.5H_2O$

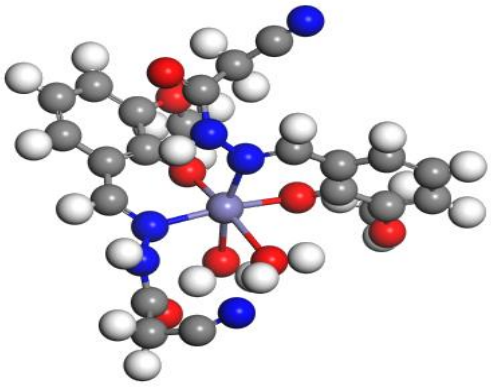

Figure 10: Molecular structure of $[Fe(HL)_2(H_2O)_2].Cl.2H_2O$

3.4.2. Quantum Chemical Reactivity Descriptors

One concept of the DFT technique is the chemical reactivity of molecular organizing, the energies related to frontier molecular orbitals (Figure 11 and 12), specifically E_{HOMO} and E_{LUMO}, as well as its band gap energy, which shows how a molecule eventually interacts via charges through charge transfer, electronegativity (χ), chemical potential (Π), electron affinity (EA), global softness (S), absolute hardness (η), and global electrophilicity index (ω) (Table 5)[18].

HOMO

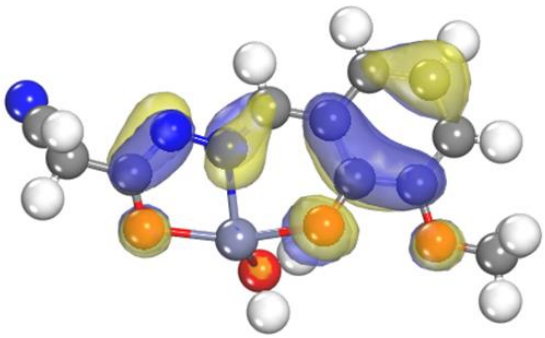

LUMO

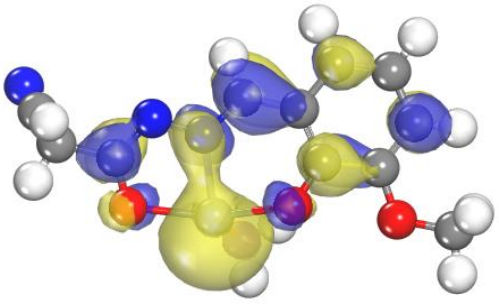

Figure 11: HOMO and LUMO for $[Zn(L)(H_2O)].0.5H_2O$

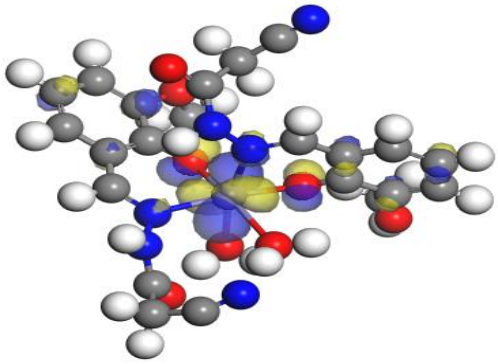

HOMO

LUMO

HO

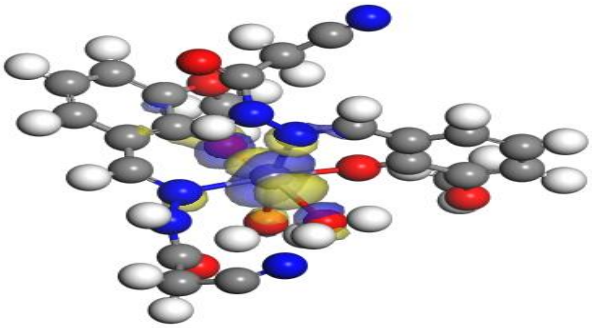

Figure 12 : HOMO and LUMO for $[Fe(HL)_2(H_2O)_2].Cl.2H_2O$

Table 5: Calculated Values of $[Zn(L)(H_2O)].0.5H_2O$ and $[Fe(HL)_2(H_2O)_2].Cl.2H_2O$ complexes

Compound	E_H (eV)	E_L ($_{eV}$)	E_H-E_L (eV)	Π (eV)	χ (eV)	η (eV)	S (eV^{-1})	Ω (eV)
$[Zn(L)(H_2O)].0.5H_2O$	-4.635	-2.407	-2.228	-3.521	3.521	1.114	0.4488	5.5643
$[Fe(HL)_2(H_2O)_2].Cl.2H_2O$	-4.319	-3.450	-0.869	-3.884	3.884	0.4345	1.1507	17.359

3.5. Biological potency

3.5.1. Antimicrobial activities :

In-vitro antibacterial screening of the examined $[Zn(L)(H_2O)].0.5H_2O$ and $[Fe(HL)_2(H_2O)_2].Cl.2H_2O$ complexes (Table 6) were examined against many types of bacteria: comprising two Gram (+ve) bacteria (Bacillus subtilis and Staphylococcus aureus), two Gram (-ve) bacteria (Escherichia coli and Klebsiella), and fungi (Candida albicans). The experimental antibacterial activity revealed the following observations:

1- $[Zn(L)(H_2O)].0.5H_2O$ complex showed antimicrobial activity against several microorganisms, with the exception of Klebsiella.

2- $[Fe(HL)_2(H_2O)_2].Cl.2H_2O$ demonstrated no activity against several microorganisms.

Table 6: The inhibitory zone in millimeters (mm) represents the antimicrobial activity of the examined $[Zn(L)(H_2O)].0.5H_2O$ and $[Fe(HL)_2(H_2O)_2].Cl.2H_2O$ complexes.

Sample	*B.subtilis*	*S.aureus*	*E.coli*	*Klebsiella*	*C.albicans*
DMSO	NA	NA	NA	NA	NA
Zn	16	14	17	NA	14
Fe	NA	NA	NA	NA	NA

3.5.2. Antioxidant Activity of DPPH:

The antioxidant activity of the substances $[Zn(L)(H_2O)].0.5H_2O$ and $[Fe(HL)_2(H_2O)_2].Cl.2H_2O$ complexes was assessed using the DPPH technique (Table 7). The findings demonstrated that these substances exhibited concentration-dependent antioxidant properties. Depending on the compounds' structures, the different examined compounds' antioxidant efficacy differed. to compare the antioxidant activity of the substances, ascorbic acid is utilized as a standard.

Table 7: DPPH (IC_{50}) of the samples under investigation.

Compounds	Ascorbic acid	Zn(II)-complex	Fe(III)-complex
IC_{50} (mg/ml)	0.0222	0.463	0.137

4. Conclusion

In this study, we synthesized Zn(II) and F(III) complexes from cyanohydrazone derivatives (H_2L) and used standard methods to characterize them. The structures of metal complexes have been optimized with the DMol3 tool from the material studio program. It was suggested that the $[Zn(L)(H_2O)].0.5H_2O$ complex had a tetrahedral structure, while the $[Fe(HL)_2\ (H_2O)_2].Cl.2H_2O$ complex had an octahedral structure. The identification of water molecules both internally and externally the coordination zone of the complex was validated

by the thermal studies. Eyring equations were utilized to ascertain the thermodynamic and kinetic parameters. According to the antibacterial properties, the Zn (II) compound is active against a variety of organisms. However, both complexes have significant antioxidant properties.

5. References

1. Hussain, R., et al., (2023) Synthesis, spectroscopic and nonlinear optical properties, and antimicrobial activity of Cu (II), Co (II), and Ni (II) complexes: experimental and theoretical studies. ACS omega,. **8**(45): p. 42598-42609.
2. Agili, F., (2024) Novel hydrazide hydrazone derivatives as Antimicrobial agents: design, synthesis, and Molecular Dynamics. Processes,. **12**(6): p. 1055.
3. Mostafa, M.M., (2021) Comparative Studies of Some Novel Cu (II) Polymeric Complexes Derived from Cyanoacetylhydrazine (CAH; L). The Role of Solvents Used on the Structure and Geometry of the Isolated Cu2+ Complexes. Open *Journal of Inorganic Chemistry*,. **11**(4): p. 111-130.
4. Murugappan, S., et al., (2024) Hydrazide-hydrazone/hydrazone as enabling linkers in anti-cancer drug discovery: A comprehensive review. *Journal of Molecular Structure*,: p. 138012.
5. Moreira, J.M., et al., (2025) Synthesis and Characterization of Novel Hydrazone Complexes: Exploring DNA/BSA Binding and Antimicrobial Potential. ACS Omega,.
6. Al-Azmi, A. and E. John, (2021) Synthesis and characterization of novel tricyanofuran hydrazone probe: solvatochromism, density-functional theory calculation and selective fluorescence, and colorimetric determination of iron (III). Luminescence,. **36**(5): p. 1220-1230.
7. Abd El-Hamid, S.M., et al., (2025) Structural, Spectroscopic, and Docking Analysis of N, O-Donor Ligand Metal Complex Nanoparticles With Hypolipidemic Effects via Lipoprotein Lipase Activation in High-Fat Diet Mice. Chemistry & Biodiversity,. **22**(5): p. e202403003.
8. Barwa, P., et al., (2024) Investigating the antimicrobial potential of diorganotin (IV) complexes incorporating hydrazone ligands: Synthesis, structural elucidation, X-ray crystallography, DFT, and antimicrobial activity. Inorganica Chimica Acta,. **564**: p. 121941.
9. Abdelrahman, M.S., et al., (2022) Synthesis, molecular modeling, and docking studies of a new pyridazinone-acid hydrazone ligand, and its nano metal complexes. Spectroscopy, thermal analysis, electrical properties, DNA cleavage, antitumor, and antimicrobial activities. *Journal of Molecular Structure*,. **1251**: p. 131947.
10. Camaioni, L., et al., (2023) Antifungal properties of hydrazine-based compounds against Candida albicans. Antibiotics,. **12**(6): p. 1043.
11. Başaran, E., et al., (2022) Synthesis, structural characterization, and biological evaluation of some hydrazone compounds as potential antioxidant agents. Russian *Journal of Bioorganic Chemistry*,. **48**(1): p. 143-152.
12. Balouiri, M., M. Sadiki, and S.K. Ibnsouda, (2016) Methods for in vitro evaluating antimicrobial activity: A review. *Journal of pharmaceutical analysis*,. **6**(2): p. 71-79.
13. Kitts, D.D., A.N. Wijewickreme, and C. Hu, (2000) Antioxidant properties of a North American ginseng extract. Molecular and cellular biochemistry,. **203**: p. 1-10.
14. Fetoh, A., et al., (2019) Synthesis, characterization, cyclic voltammetry and biological studies of Zn (II), Cd (II), Hg (II) and UO22+ complexes of thiosemicarbazone salt. Applied Organometallic Chemistry,. **33**(4): p. e4787.
15. Sarkar, S. and K. Dey, (2005) Synthesis and spectroscopic characterization of some transition metal complexes of a new hexadentate N2S2O2 Schiff base ligand. Spectrochimica Acta Part A: Molecular and Biomolecular Spectroscopy,. **62**(1-3): p. 383-393.
16. Coats, A.W. and J. Redfern, (1964) Kinetic parameters from

thermogravimetric data. Nature,. **201**(4914): p. 68-69.
17. Horowitz, H., Metzer. G. (1963) Esso Res Engg Co., Linden, NJ. *J Anal Chem,*. **35**: p. 1464.
18. Mohammed, M.A., et al., (2023) Fabrication of novel Fe (III), Co (II), Hg (II), and Pd (II) complexes based on water-soluble ligand (NaH2PH): structural characterization, cyclic voltammetric, powder X-ray diffraction, zeta potential, and biological studies. Applied Organometallic Chemistry,. **37**(1): p. e6910.